ISSN 1674-1056
http://cpb.iphy.ac.cn
http://iopscience.iop.org/cpb
中国物理 B
Chinese Physics
中国物理 Chinese Physics B

Shannon information entropies for rectangular multiple quantum well systems with constant total lengths

M.Solaimani, Guo-Hua Sun(孙国华), Shi-Hai Dong(董世海)
Citation: Chin. Phys. B . 2018, 27(4): 040301. **doi:** 10.1088/1674-1056/27/4/040301

Journal homepage: http://cpb.iphy.ac.cn; http://iopscience.iop.org/cpb

What follows is a list of articles you may be interested in

Nuclear magnetic resonance for quantum computing: Techniques and recent achievements

Tao Xin(辛涛), Bi-Xue Wang(王碧雪), Ke-Ren Li(李可仁), Xiang-Yu Kong(孔祥宇), Shi-Jie Wei(魏世杰), Tao Wang(王涛), Dong Ruan(阮东), Gui-Lu Long(龙桂鲁)
Chin. Phys. B . 2018, 27(2): 020308. **doi:** 10.1088/1674-1056/27/2/020308

Analytical and numerical investigations of displaced thermal state evolutions in a laser process

Chuan-Xun Du(杜传勋), Xiang-Guo Meng(孟祥国), Ran Zhang(张冉), Ji-Suo Wang(王继锁)
Chin. Phys. B . 2017, 26(12): 120301. **doi:** 10.1088/1674-1056/26/12/120301

A new two-mode thermo-and squeezing-mixed optical field

Jun Zhou(周军), Hong-yi Fan(范洪义), Jun Song(宋军)
Chin. Phys. B . 2017, 26(7): 070301. **doi:** 10.1088/1674-1056/26/7/070301

Solvability of a class of *PT*-symmetric non-Hermitian Hamiltonians: Bethe ansatz method

M Baradaran, H Panahi
Chin. Phys. B . 2017, 26(6): 060301. **doi:** 10.1088/1674-1056/26/6/060301

New approach for anti-normally and normally ordering bosonic-operator functions in quantum optics

Shi-Min Xu(徐世民), Yun-Hai Zhang(张运海), Xing-Lei Xu(徐兴磊), Hong-Qi Li(李洪奇), Ji-Suo Wang(王继锁)
Chin. Phys. B . 2016, 25(12): 120301. **doi:** 10.1088/1674-1056/25/12/120301

Shannon information entropies for rectangular multiple quantum well systems with constant total lengths*

M Solaimani[1,†], Guo-Hua Sun(孙国华)[2], and Shi-Hai Dong(董世海)[3,‡]

[1] Department of Physics, Faculty of Science, Qom University of Technology, Qom, Iran
[2] Catedrática CONACyT, CIC, Instituto Politécnico Nacional, Unidad Profesional ALM, CDMX, C. P. 07700, Mexico
[3] Laboratorio de Información Cuántica, CIDETEC, Instituto Politécnico Nacional, Unidad Profesional ALM, CDMX, C. P. 07700, Mexico

(Received 26 October 2017; revised manuscript received 22 December 2017; published online 10 March 2018)

We first study the Shannon information entropies of constant total length multiple quantum well systems and then explore the effects of the number of wells and confining potential depth on position and momentum information entropy density as well as the corresponding Shannon entropy. We find that for small full width at half maximum (FWHM) of the position entropy density, the FWHM of the momentum entropy density is large and *vice versa*. By increasing the confined potential depth, the FWHM of the position entropy density decreases while the FWHM of the momentum entropy density increases. By increasing the potential depth, the frequency of the position entropy density oscillation within the quantum barrier decreases while that of the position entropy density oscillation within the quantum well increases. By increasing the number of wells, the frequency of the position entropy density oscillation decreases inside the barriers while it increases inside the quantum well. As an example, we might localize the ground state as well as the position entropy densities of the 1st, 2nd, and 6th excited states for a four-well quantum system. Also, we verify the Bialynicki–Birula–Mycieslki (BBM) inequality.

Keywords: position and momentum Shannon entropies, multiple quantum well, entropy densities

PACS: 03.65.–w, 03.65.Ge, 03.67.–a **DOI:** 10.1088/1674-1056/27/4/040301

1. Introduction

Shannon in his classical paper[1] reported the fundamental limits to signal processing operations such as reliable storing and communicating data and limits to compressing data. Thereafter, this theory was found to have other applications such as cryptography, quantum computing, thermal physics, atomic and molecular structure, etc. This is the so-called Shannon entropy, which is a measure of a random variable uncertainty and can also become the expected value of the information existing in a message.

During the last few decades, the Shannon entropies have been analytically calculated for low-lying states of some quantum systems with potentials such as the Morse potential,[2,3] harmonic oscillator,[4,5] the Pöschl–Teller potential,[2,6] modified Yukawa potential,[7] and the Rosen–Morse potential.[8] On the other hand, the Shannon entropies for other complicated quantum systems such as the position-dependent mass Schrödinger equation with null potential,[9] quantum dots,[10] double-well potential,[11] finite well,[12] and infinite circular well[13] have also been investigated. Relevant studies about this topic were also conducted in Refs. [14]–[17].

In addition to their intrinsic interest, the entropic uncertainty relations[4] have been widely used to reproduce the charge and momentum densities of the atomic and molecular systems[18] and also to investigate the squeezing localization.[19] The electronic localization properties of the system can be used for designing low-dimensional electron nano-devices and also electromagnetic waveguides with predetermined transport properties. The most widely studied potential models are one-dimensional (1D) quasi-periodic systems, such as the slowly varying potential,[20] Harper model,[21] and the complex quasi-periodic potential ones.[22]

Periodic structures of layers of two or more materials can construct a superlattice. The thickness of each layer is usually several nanometers. Different types of building blocks such as Fibonacci[23] and Pascal-type[24] possess some physical properties that are more appropriate for developing quantum devices. Our approach to the building of a superlattice or multiple quantum well system is based on retaining the total length of the structure constant and simultaneously changing the number of quantum wells. In this way, the smaller nano-device sizes in addition to better physical properties are accessible. So far, we have studied the optical properties of constant total effective length multiple quantum well systems,[25] the physical properties of GaN/AlN constant total effective radius multi-well quantum rings under well number variation effects,[26] and the optical properties of two-electron[27] and impurity including[28] GaN/AlN constant total effective radius multi-shell quantum rings and dots. And we also have studied the miniband formation scenario in GaN/AlN constant total

*Project supported by the Iranian Nanotechnology Initiative Council (INIC), the 20180677-SIP-IPN, Mexico, and the CONACYT 288856-CB-2016, Mexico.
†Corresponding author. E-mail: solaimani.mehdi@gmail.com; solaimani@qut.ac.ir
‡Corresponding author. E-mail: dongsh2@yahoo.com
© 2018 Chinese Physical Society and IOP Publishing Ltd

effective length multiple quantum dots.[29]

It should be recognized that the above-mentioned studies of the Shannon entropy focus on the soluble quantum systems,[2–13] which means that the solutions of those quantum systems are analytical and consequently the wave function in momentum space can be calculated by the Fourier transform. In the present work, we study the quantum information entropies for rectangular multiple quantum well systems with a constant total length, in which the solution cannot be obtained analytically. We will obtain the position and momentum information entropy densities and the Shannon entropies for some constant total effective length multiple quantum wells through a numerical approach. We discuss the effects of the numbers of wells (1, 2, 3, 4, 15, and 22) and confined potential depth on the entropies and entropy densities for the ground state and the 1st, 2nd, 6th, and 50th states.

2. Formalism

We start with a 1D time-independent Schrödinger equation

$$\left(-\frac{\hbar^2}{2m}\frac{\mathrm{d}^2}{\mathrm{d}x^2}+V(x)\right)\psi(x)=E\psi(x), \tag{1}$$

where the geometrical confining potential $V(r)$ is defined as,[21–25]

$$V(r)=\begin{cases} V_{\text{conf}} & i=1,3,\ldots \\ 0, & i=2,4,\ldots; \end{cases} \quad \frac{i-1}{2N+1}L_{\text{eff}}<r<\frac{i}{2N+1}L_{\text{eff}}. \tag{2}$$

Here, V_{conf} is a constant relative conduction band offset and the notation i represents the i-th well or barrier in the studied system. In this work, we assume that the well width and the barrier width are equal. The energies E_n and the normalized wave functions $\psi_n(x)$ can be calculated through a numerical discretization technique.[30]

The position and momentum space information entropies S_x and S_p are related to the Shannon information entropy densities $\rho_s(x)$ and $\rho_s(p)$ defined as[8,9,11]

$$\rho_s(x)=|\psi(x)|^2\ln(|\psi(x)|^2), \tag{3a}$$

$$\rho_s(p)=|\varphi(p)|^2\ln(|\varphi(p)|^2). \tag{3b}$$

The position and momentum space information Shannon entropies S_x and S_p are written respectively as

$$S_x=-\int_{-\infty}^{+\infty}|\psi(x)|^2\ln(|\psi(x)|^2)\,\mathrm{d}x=-\int_{-\infty}^{+\infty}\rho_s(x)\,\mathrm{d}x, \tag{4a}$$

$$S_p=-\int_{-\infty}^{+\infty}|\varphi(p)|^2\ln(|\varphi(p)|^2)\,\mathrm{d}x=-\int_{-\infty}^{+\infty}\rho_s(p)\,\mathrm{d}p, \tag{4b}$$

where $\psi(x)$ is the normalized wave function in position space and can be obtained through the numerical solution to Eq. (1). The $\varphi(p)$ is the normalized wave function in momentum space and can be calculated by the Fourier transform as

$$\varphi(p)=\frac{1}{\sqrt{2\pi}}\int\psi(x)\,\mathrm{e}^{-\mathrm{i}px}\,\mathrm{d}x. \tag{5}$$

In this work, however, we calculate it by using the fast Fourier transform (FFT) method. Note that because of the logarithmic factors in the integrals, Shannon entropies (4) become rather difficult to solve analytically even for quantum systems. As a result, we have to perform the integrals numerically for the present case. The entropic uncertainty relation obtained by Beckner, BBM, is given by

$$S_x+S_p\geq D(1+\ln\pi), \tag{6}$$

where D denotes the spatial dimension and here we take $D=1$.

3. Results and discussion

We investigate the constant total effective length multiple quantum well systems with equally spaced quantum wells and barriers. If the total system length in our system is 60 nm, then the width of each well and barrier in a double quantum well system with constant 60 nm in total length is given by $60/5=12$ nm, in which there are two wells and three barriers, which are equally spaced between each other.

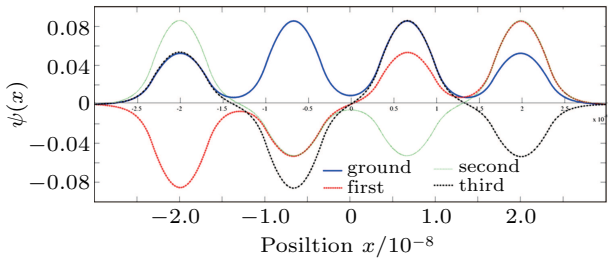


Fig. 1. (color online) Normalized wave functions as a function of position x for a four-quantum well system.

At the first step, in Fig. 1 we plot some normalized wave functions as a function of position x for a four-well system. This figure clearly shows that the curves are consistent with the node theorem of wave functions, i.e., the 3rd excited state has three nodes. Then, in order to study the entropy distributions for the quantum wells and barriers, we plot the position and momentum space entropy densities for different circumstances. In Fig. 2 we present the variations of the position and momentum entropy densities with position x for a single quantum well. The total system length is assumed to be 60 nm. The blue solid line, green dashed line, black dotted line, and purple dash–dotted line represent the position and momentum entropy densities for the normalized ground state, 1st, 2nd, and 6th excited states, respectively. Panels (a)–(f) illustrate different confined potential depths. Note that in all systems the position entropy densities for the ground state, 1st, and 2nd excited states are sensible only inside the quantum well. However, for the systems each with a small depth of the quantum well, e.g. panel (a), the maximum position entropy densities occur inside the barriers (see the purple dash-dotted line in

panel (a)). Also, notice that by increasing the well depth (see panels (c) and (e)), the position entropy density of the 6th excited state in the barrier decreases and its value in the quantum well increases. Comparing the position entropy densities with the corresponding momentum entropy densities, it is found that for the smaller FWHM of the position entropy density, the FWHM of the momentum entropy density becomes larger and vice versa. To see this clearly, for the position entropy density of the ground state, we compare the solid blue lines in panels (a) and (b) and those in panels (e) and (f). This fact is also true for the position and momentum entropy densities of other excited states. In the meantime, by increasing the potential depth the FWHM of the position entropy density decreases, but the FWHM of the momentum entropy density increases.

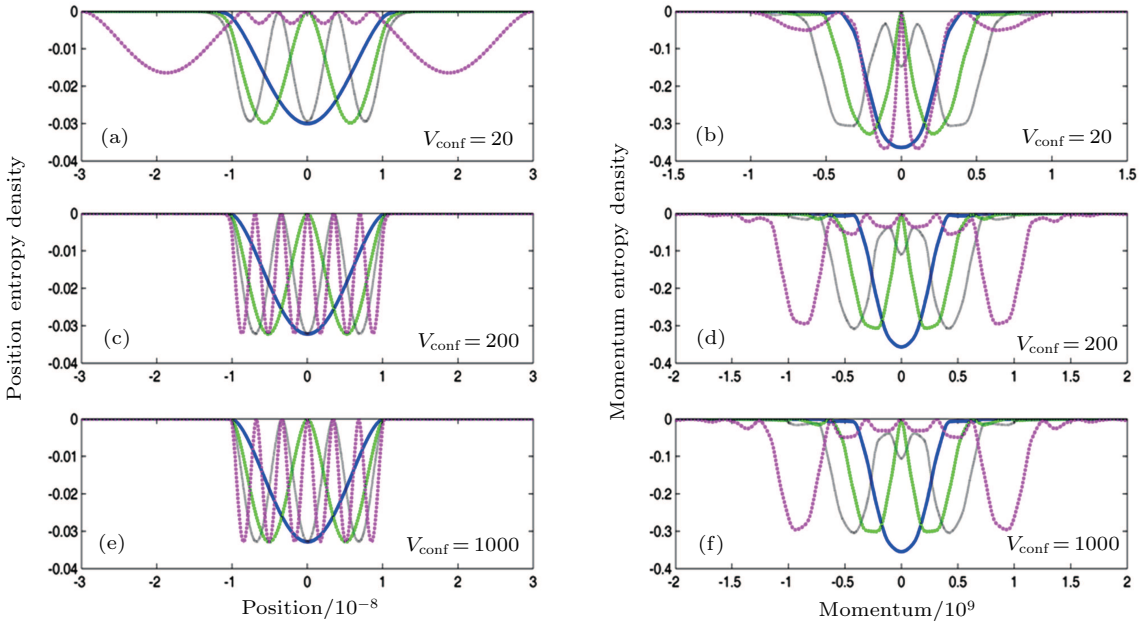


Fig. 2. (color online) Variations of the position and momentum entropy densities with position x and momentum p for a single-quantum well system. The total system length is 60 nm. The blue solid line, green dashed line, black dotted line, and purple dash-dotted line denote the position and momentum entropy densities for the normalized ground state, 1st, 2nd, and 6th excited states, respectively. Panels (a)–(f) are plotted for different confined potential depths.

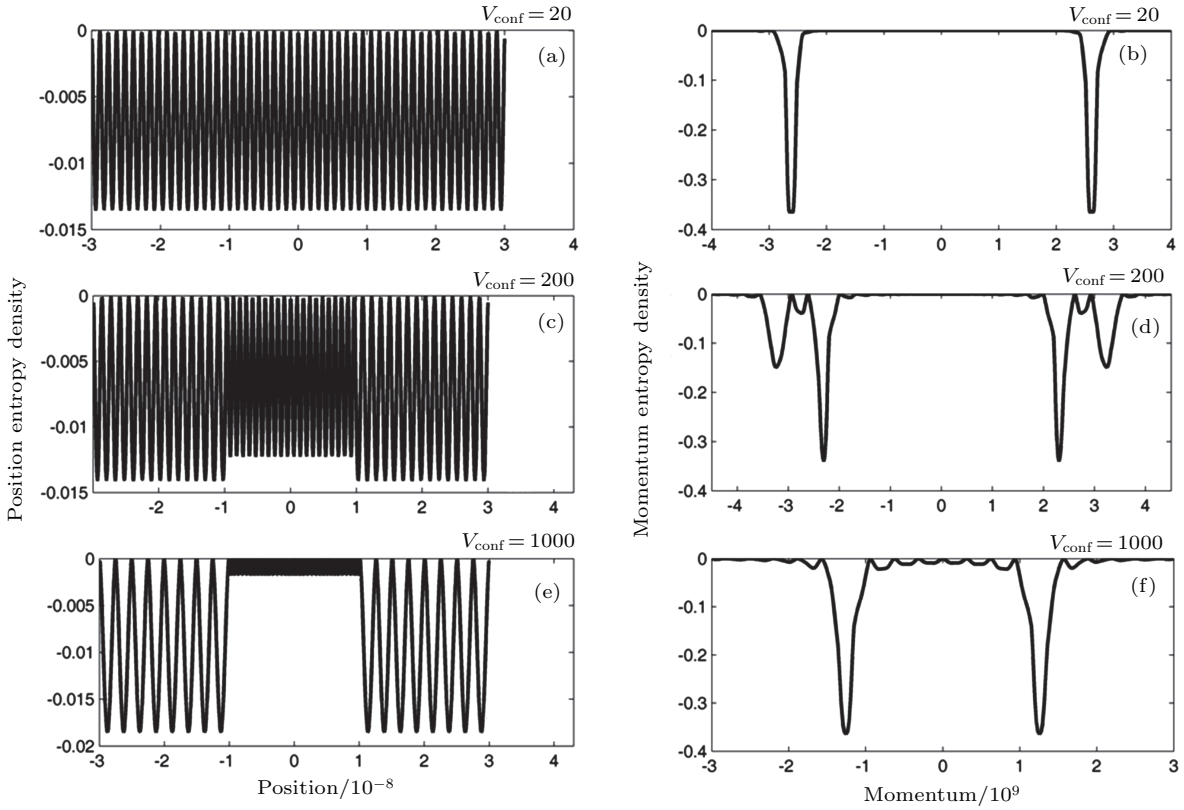


Fig. 3. The same as Fig. 2. The black solid line denotes the normalized 50th excited state.

On the other hand, to observe the effects of the confined potential on the position and momentum entropy density of a high excited state for a single quantum well, we plot the variations of the position and momentum entropy densities with position x for a single quantum well in Fig. 3. The total system length is again assumed to be 60 nm. The black solid line shows the position and momentum entropy densities of the 50th excited state. Figures 3(a)–3(f) show the cases of different confined potential depths. It is interesting to find that in Fig. 3(a), where the confined potential depth is small (20 meV), the position entropy density of the 50th state is distributed uniformly inside the total length of the system. However, by increasing the potential depth (see Figs. 3(c) and 3(e)), this uniform distribution shall be broken and gradually the position entropy density inside the well decreases. A comparison between the position and corresponding momentum entropy densities shows that if the position entropy density is distributed inside a wide position space interval, the corresponding momentum entropy density will be localized in a narrow interval of the momentum space. However, for an intermediate confined potential depth (see Figs. 3(c) and 3(d)), the momentum space entropy density has the widest interval of distribution. Finally, we see that by increasing the confined potential depth, the frequency of the position entropy density oscillation inside the quantum barriers decreases, while the frequency of the position entropy density oscillation inside the quantum wells increases.

Now, we increase the number of wells to 2 and obtain the results as shown in Figs. 4 and 5. In our double quantum well system we keep the 60 nm total length constant (60 nm). Unlike the scenario in Fig. 2, in this system the position entropy densities for all the ground state, 1st, 2nd, and other excited states are localized inside the quantum wells. For double well systems with small confined potential depth panel (Fig. 5(a)), the distributions of the position entropy densities inside the quantum wells are identical. Notice the different lines inside the two wells. However, by increasing the confined potential depth to 200 meV (Fig. 5(c)), these identical distributions between quantum wells are destroyed. In Fig. 5(c), the maximum position entropy density of the 1st excited state occurs in the left quantum well, maximum position entropy density of the 2nd excited state occurs in the right quantum well and maximum position entropy density of the 6th excited state occurs in the left well. This scenario is also true for Fig. 5(e) with larger confined potential depth (1000 meV). In the meantime, for the corresponding momentum information entropies we find that although a position entropy density may be asymmetric with respect to the origin (one quantum well may have larger position entropy density, e.g., the one represented with the black dotted line in the panel (c)), the corresponding momentum information entropy is symmetric with respect to the origin.

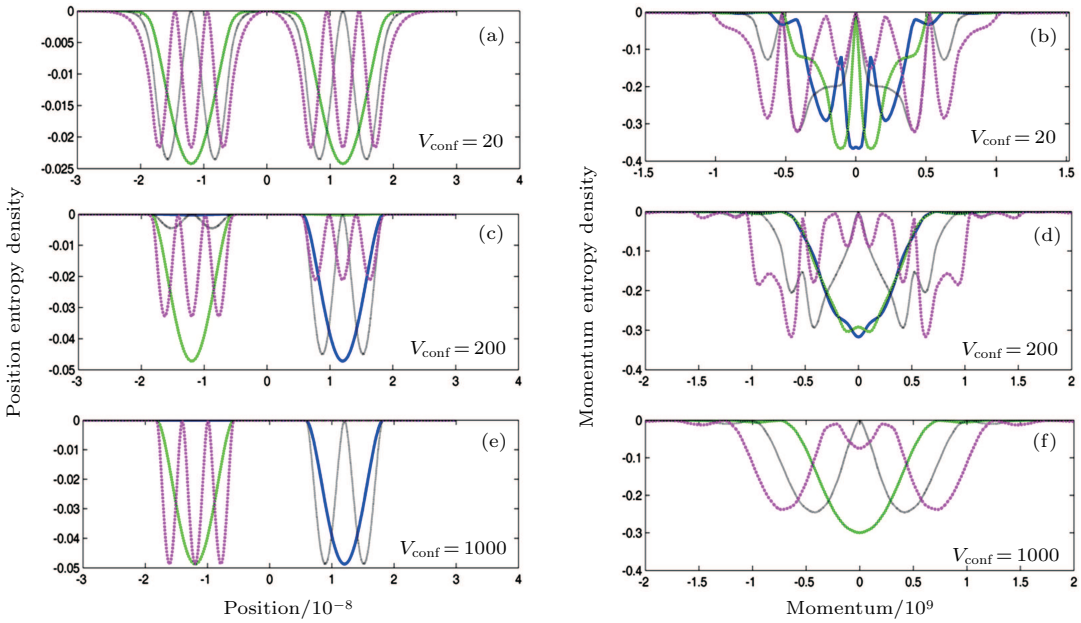


Fig. 4. (color online) The same as Fig. 2, but for a double-quantum-well system with 60 nm in total length.

We now study the effects of the confined potential on the position and momentum entropy densities of the 50th excited state for the double quantum well system. Unlike the scenario in Fig. 3(a), the distributions of the position entropy of small confined potential depth (20 meV) of the 50th excited state for a double quantum well system in Fig. 5(a) are not completely uniform. However, the value of the position information entropy inside the quantum wells is smaller than inside the quantum barriers. But by increasing the confined potential depth up to an intermediate value (200 meV, Fig. 5(c)), we find that the value of the position entropy density is uniform inside the whole system except inside the central quantum barrier in

which its value is larger. Our previously mentioned issue about the frequency of position entropy density oscillation for a single quantum well system is still true for the double quantum well system. Here, however, there is another fact. By increasing the number of wells (comparing Fig. 3(e) with Fig. 5(e)), the frequency of position entropy density oscillation decreases inside the barriers and increases inside the quantum wells. Finally, we note that in Figs. 5(a), 5(c), and 5(e) the amplitude of the position entropy density inside the central quantum barrier increases with confined potential depth increasing.

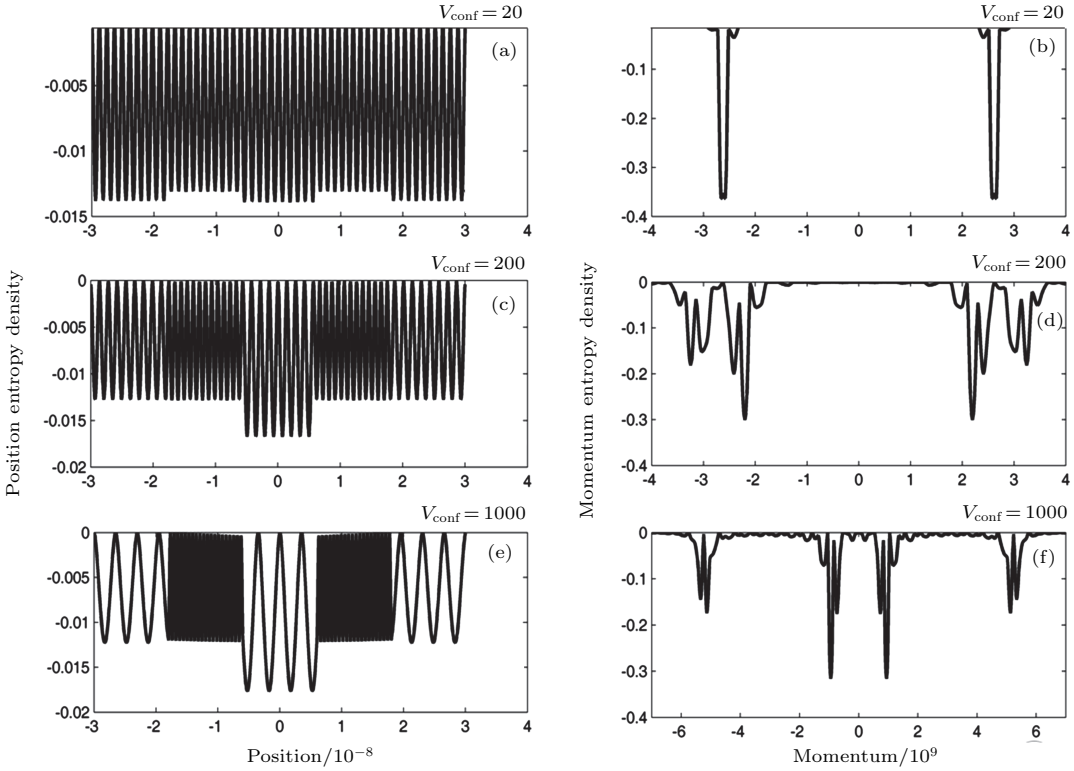


Fig. 5. The same as Fig. 3, but for a double-quantum-well system with 60 nm in total length.

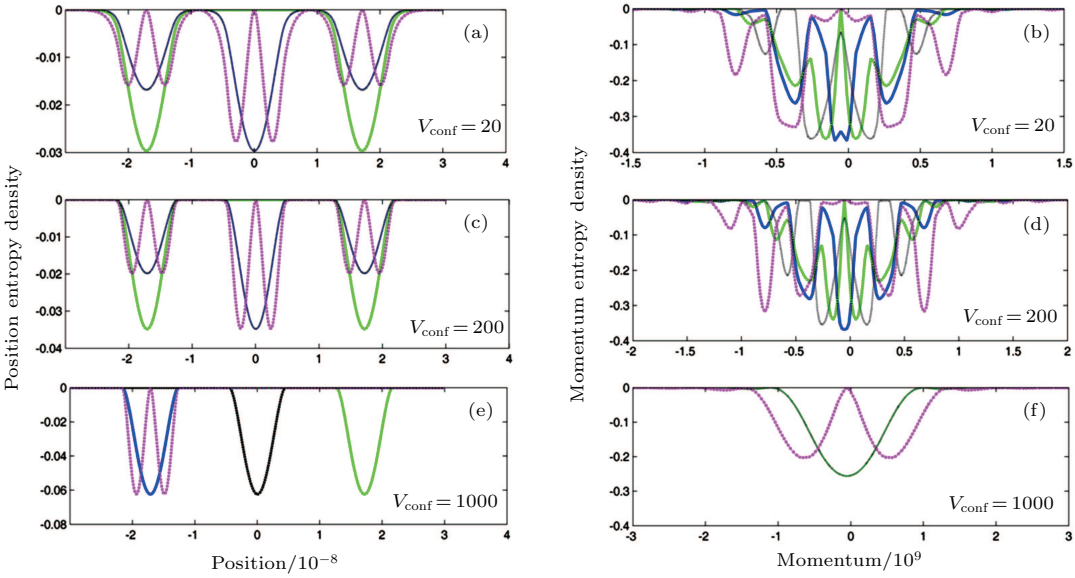


Fig. 6. (color online) The same as Fig. 2, but for a triple-quantum-well system with 60 nm in total length.

For more illustrations, we increase the number of wells up to 3 and 4. Then, we repeat the Figs. 2 and 3. The results are displayed in Figs. 6, 7, 8, and 9. Unlike the scenarios in Figs. 3 and 5, in Fig. 7, the maximum amplitude of the position entropy density is not related to the central quantum barrier. Here, there are two maxima due to the quantum barrier, which are localized at the two ends of the system. The situation for a 4-well system (see Fig. 9) is again different and two other quantum barriers have the maximum amplitudes. Roughly speaking, there is not a general statement about the

barrier which has a maximum position entropy density. Each desired quantum system has to be analyzed individually. Figure 8(e) is also interesting. In this figure, the position entropy densities of different four states (ground state, the 1st, 2nd, and 6th excited states) each are localized inside a distinct quantum well.

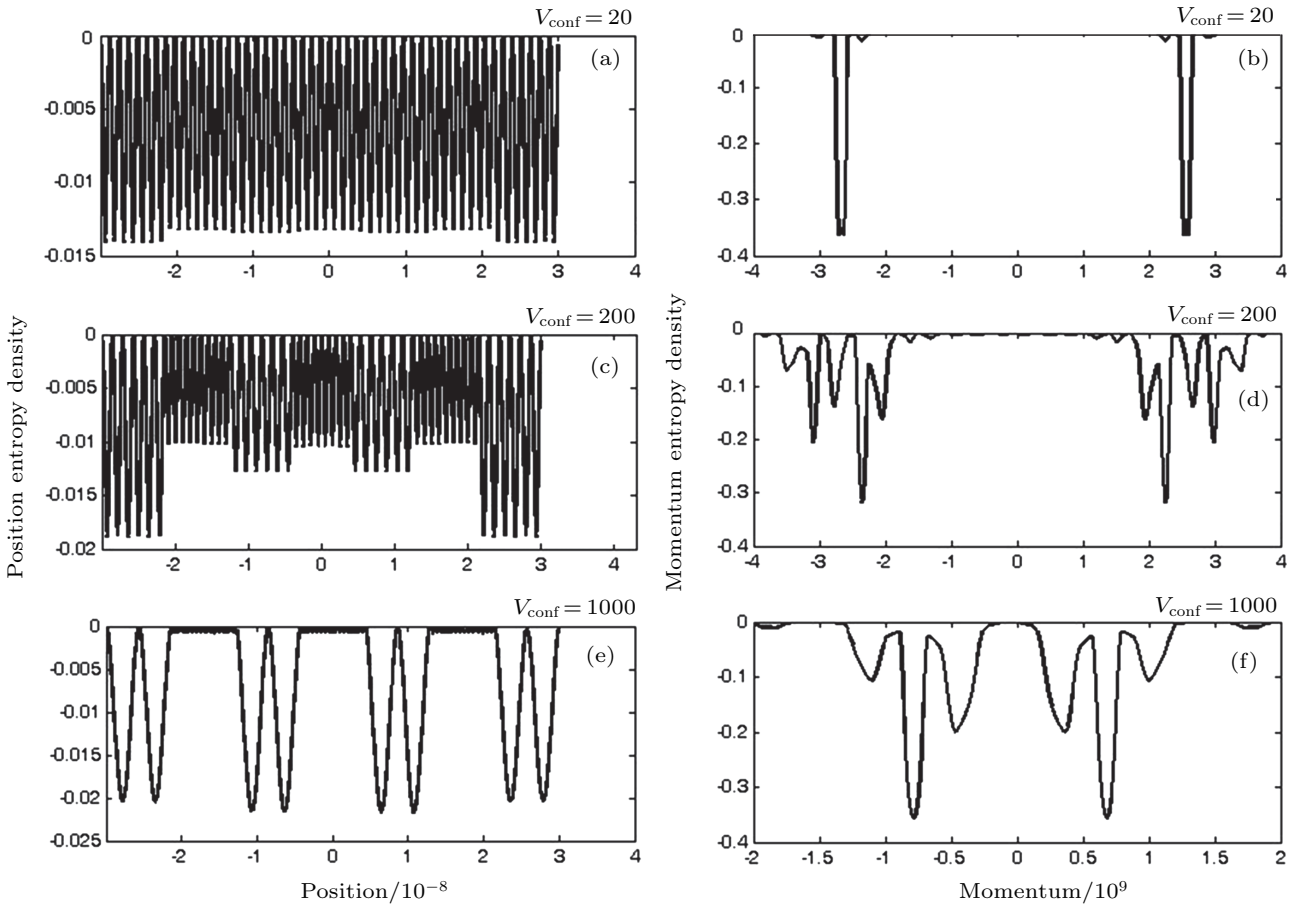


Fig. 7. The same as Fig. 3, but for a triple-quantum-well system.

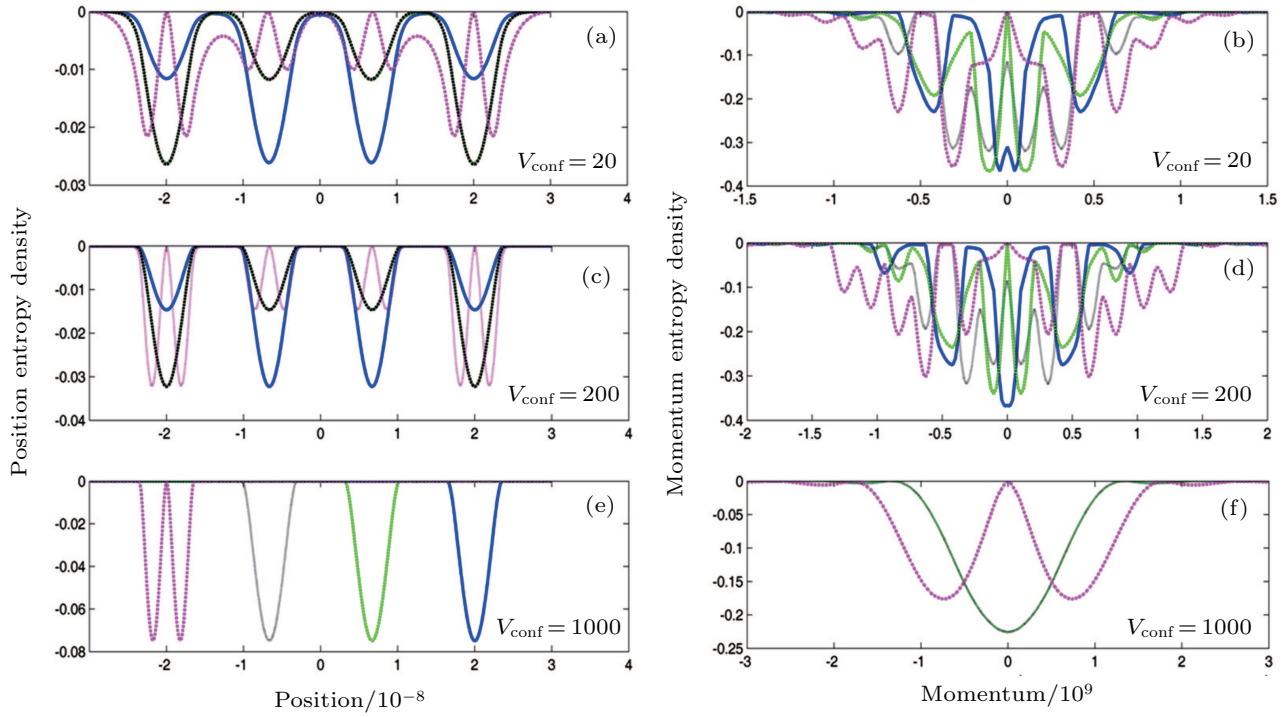


Fig. 8. (color online) The same as Fig. 2, but for a four-quantum-well system with 60 nm in total length.

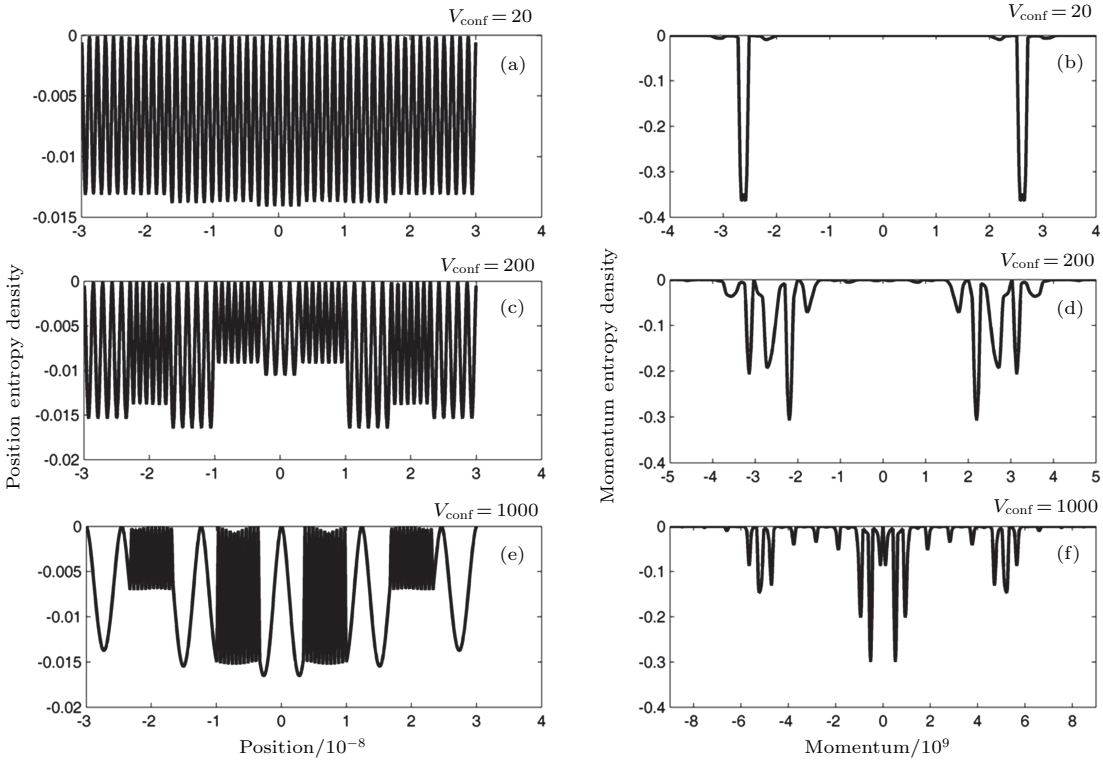


Fig. 9. The same as Fig. 3, but for a four-quantum-well system with 60 nm in total length.

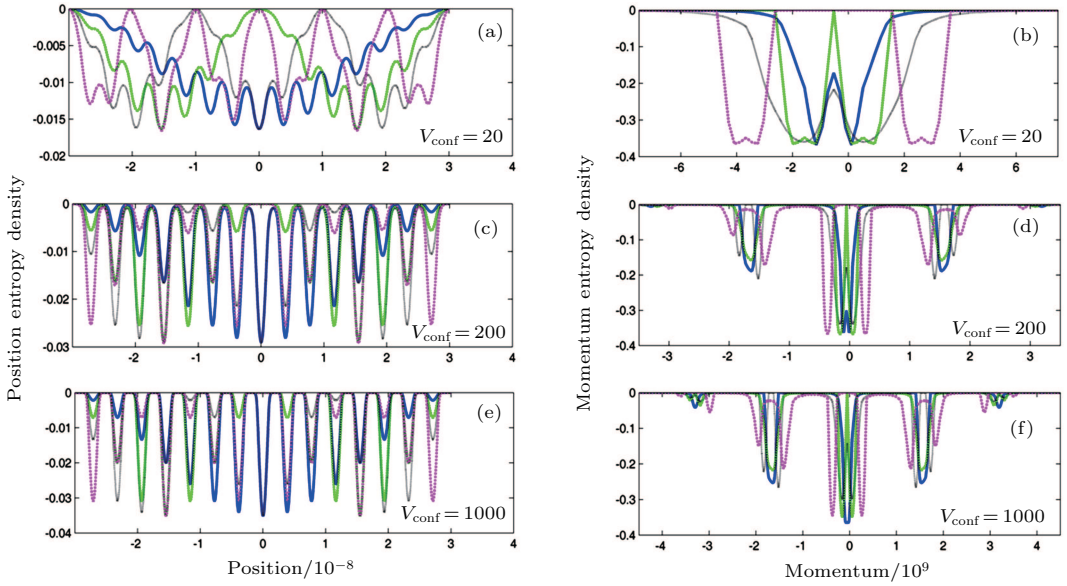


Fig. 10. (color online) The same as Fig. 2, but for a 15-quantum-well system with 60 nm in total length.

In addition, we explore two extra systems with larger numbers of wells i.e., 15 and 22. The results are shown in Figs. 10, 11, 12, and 13, respectively. At this stage, the number of wells is so large that the over system exhibits a behavior like a single quantum well with a length of 60 nm. But, there are additional oscillations in the position entropy densities as indicated with the blue solid line in Figs. 10 and 12. This behavior is very similar to that of the ground state position entropy density (blue solid line) in Fig. 2(a), in which the position entropy density is in the Gaussian form inside the quantum well. To see this similarity more clearly, one may compare the position entropy densities associated with other excited states as shown with dashed, dotted, and dash-dotted lines in Figs. 2(a), 10(a), and 12(a). In the meantime, it is clear from Figs. 10(a), 10(c), 10(e), 12(a), 12(c), and 12(e) that by increasing the confined potential depth the value of the position entropy density inside the barriers vanishes. This is because the probability of the particle staying in the barriers with infinite height is infinitesimal. Finally, we note that because the position entropy density is widely distributed inside the total position effective length, the momentum entropy density is localized in a narrow interval of the momentum in the momentum space.

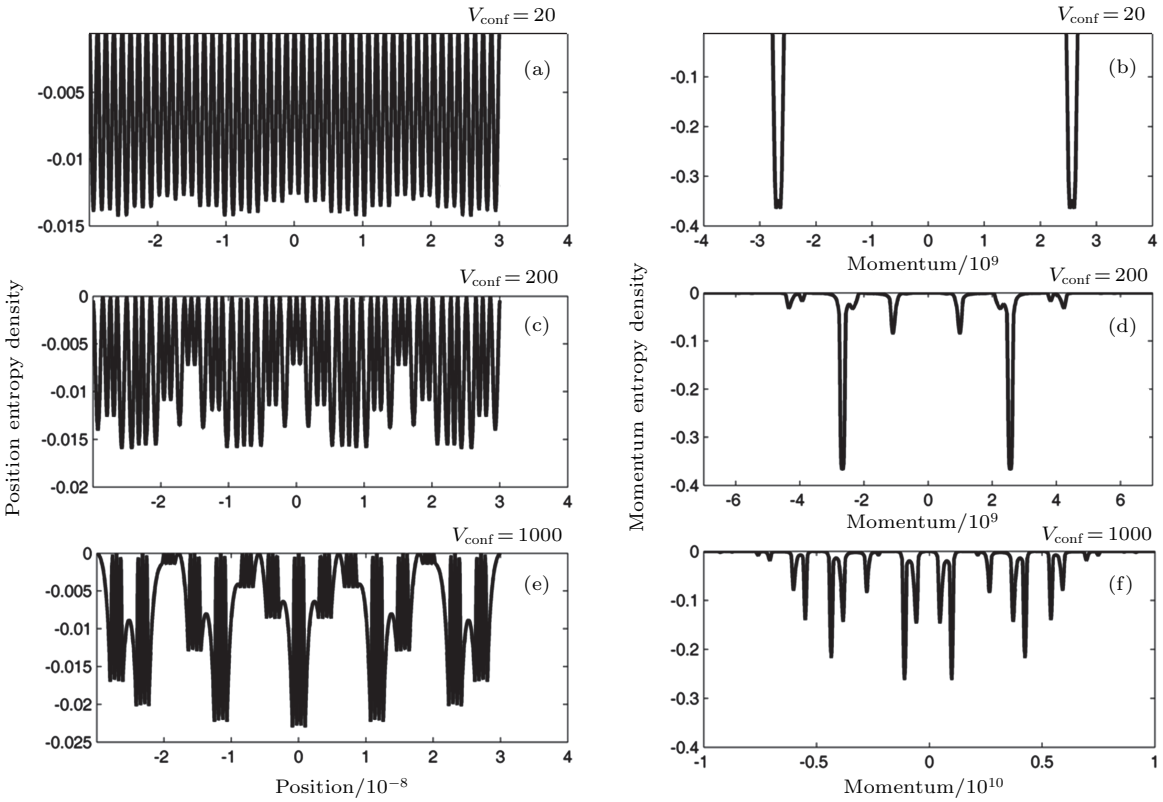


Fig. 11. The same as Fig. 3, but for a 15-quantum-well system with 60 nm in total length.

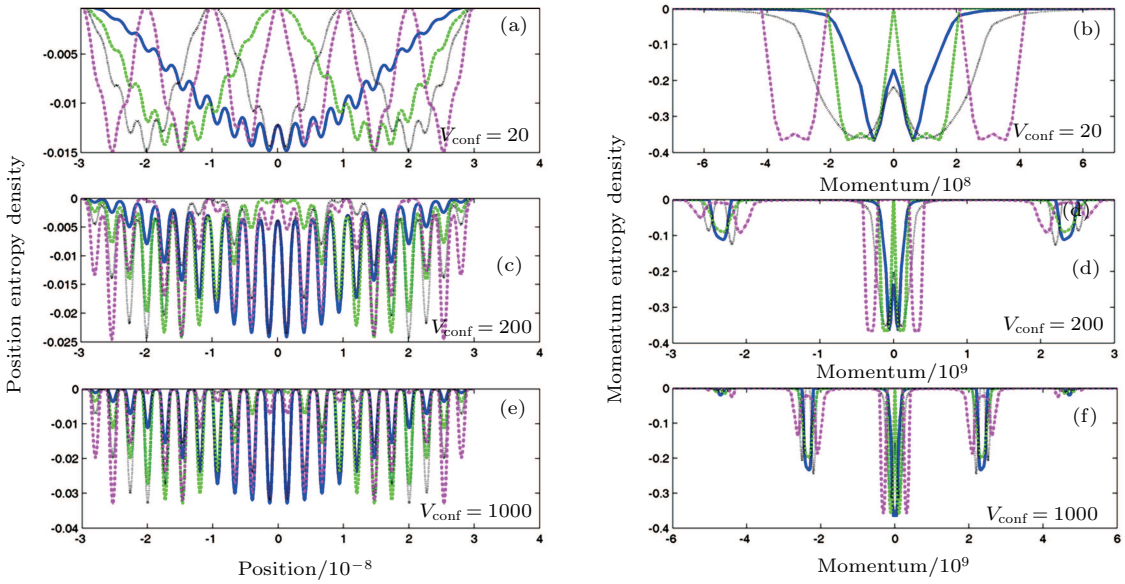


Fig. 12. (color online) The same as Fig. 2, but for a 22-quantum-well system with 60 nm in total length.

Finally, in order to study the behaviors of the position and momentum entropies and also to explore whether the BBM inequality is satisfied, we plot the variations of the position entropies with confined potential depth 'V_{conf}' as is shown in Fig. 14. Figure 14(b) is the same as Fig. 14(a) except the plot of momentum entropy. Figure 14(c) also shows the sum of the momentum and position entropies as a function of the confined potential depth "V_{conf}". As can be seen clearly from Figs. 14(a) and 14(b), as V_{conf} increases the position entropies decrease and at the same time the momentum entropies increase. However, the single well system has much smaller position and momentum entropies. To check the BBM inequality, we examine Fig. 14(c). From Figs. 14(a) and 14(b) we see that when one entropy increases the other entropy decreases. However, their sum stays above a lower bound with a value $(1+\ln(\pi)) = 2.1447$. Thus, the BBM inequality is shown to be satisfied.

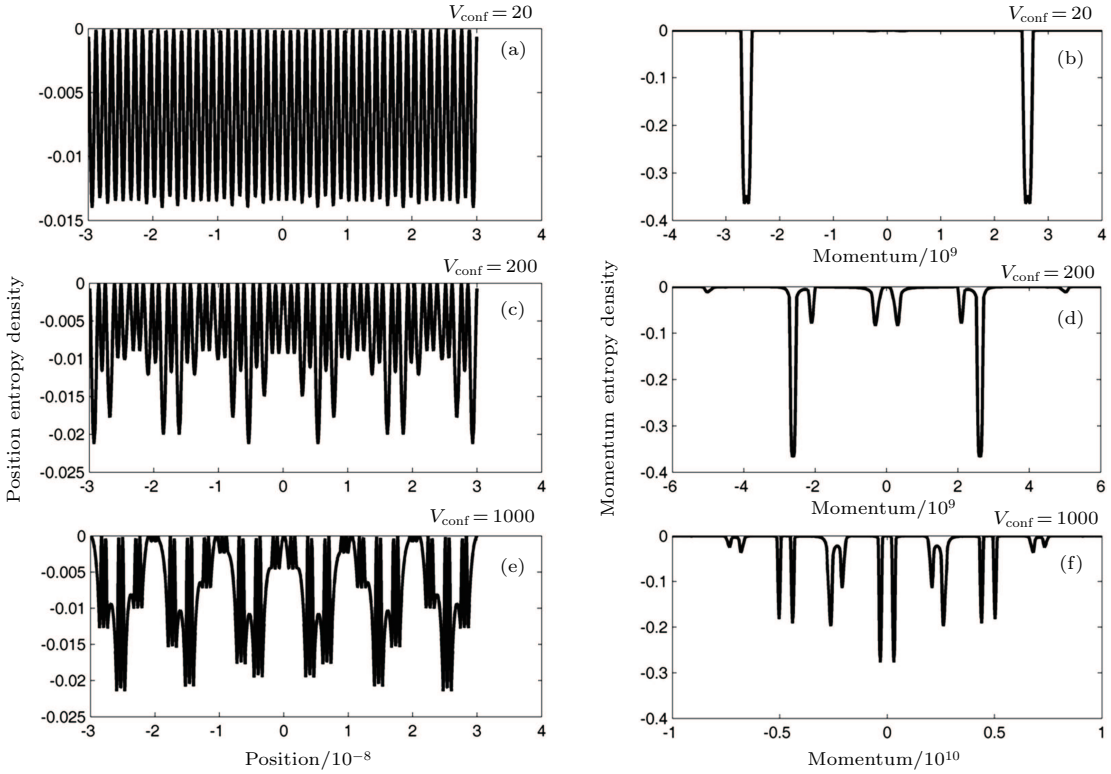


Fig. 13. The same as Fig. 3, but for a 22-quantum-well system with 60 nm in total length.

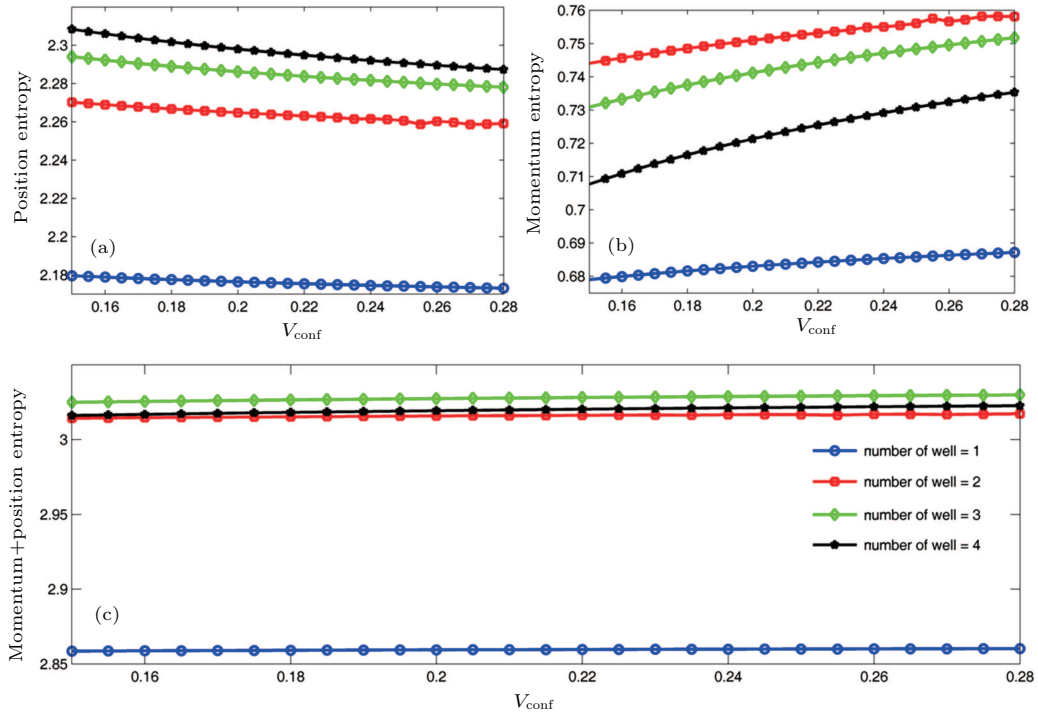


Fig. 14. (color online) Variations of (a) position, (b) momentum, and (c) sum of the position and momentum entropies with confining potential depth 'V_{conf}', respectively.

4. Conclusions

In this work we investigate the position and momentum information entropy densities in addition to position and momentum information entropies of constant total effective length multiple quantum well systems. We find that in single quantum wells, for all well depths the ground state, 1st and 2nd excited state, the position entropy densities are sensible only within the well, while for the 6th excited state, by increasing the well depth, the position entropy density in the barriers decreases and its value in the quantum well increases. For the small FWHM of the position entropy density, we have increased the FWHM of the momentum entropy density and vice

versa. For the single quantum well, by increasing the potential depth, the 50th state position entropy density within the well gradually decreases. Here, by increasing the potential depth, the FWHM of the position entropy density decreases and the FWHM of the momentum entropy density increases. For an intermediate confined potential depth of 200 meV, the momentum space entropy density has the widest interval of distribution. By increasing the potential depth, the frequency of the position entropy density oscillation inside the quantum barriers decreases and the frequency of the position entropy density oscillation inside the quantum wells increases. By increasing the number of wells, the frequency of position entropy density oscillation decreases within the barriers and it increases inside the quantum wells. In a four-well quantum system we are able to localize the ground state, 1st, 2nd, and 6th excited state position entropy densities inside a distinct quantum well. Finally, we find that the BBM inequality is satisfied. Thus, by modifying the number of wells and the potential depth we can describe the localization positions and values of the position and momentum information entropies.

References

[1] Shannon C E 1948 *Bell Syst. Tech. J.* **27** 379
[2] Dehesa J S, Martinez-Finkelshtein A and Sorokin V N 2006 *Mol. Phys.* **104** 613
[3] Aydiner E, Orta C and Sever R 2008 *Int. J. Mod. Phys. B* **22** 231
[4] Yañez R J, van Assche W and Dehesa J S 1994 *Phys. Rev. A* **50** 3065
[5] Majernik V and Opatrny T 1996 *J. Phys. A* **29** 2187
[6] Coffey M W 2007 *Can. J. Phys.* **85** 733
[7] Patil S H and Sen K D 2007 *Int. J. Quantum Chem.* **107** 1864
[8] Sun G H and Dong S H 2013 *Phys. Scr.* **87** 045003
[9] Yañez-Navarro G, Sun G H, Dytrich T, Launey K D, Dong S H and Draayer J P 2014 *Ann. Phys.* **348** 153
[10] Hazra R K, Ghosh M and Bhattacharyya S P 2008 *Chem. Phys. Lett.* **460** 209
[11] Sun G H, Dong S H, Launey K D, Dytrych T and Draayer J P 2015 *Int. J. Quantum Chem.* **115** 891
[12] Majernik V and Majernikova E 2002 *J. Phys. A* **35** 5751
[13] Song X D, Sun G H and Dong S H 2015 *Phys. Lett. A* **379** 1402
[14] Sun G H, Popov D, Camacho-Nieto O and Dong S H 2015 *Chin. Phys. B* **24** 100303
[15] Sun G H, Dong S H and Saad N 2013 *Ann. Phys.* **525** 934
[16] Sun G H, Avila Aoki M and Dong S H 2013 *Chin. Phys. B* **22** 050302
[17] Song X D, Dong S H and Zhang Y 2016 *Chin. Phys. B* **25** 050302
[18] Angulo J C, Antolin J, Zarzo A and Cuchi J C 1999 *Eur. Phys. J. D* **7** 479
[19] Orlowski A 1997 *Phys. Rev. A* **56** 2545
[20] Das Sarma S, He S and Xie X C 1988 *Phys. Rev. Lett.* **61** 2144
[21] Zhang L, Gong L Y and Tong P Q 2011 *Eur. Phys. J. B* **80** 485
[22] Hiramoto H and Kohmoto M 1989 *Phys. Rev. Lett.* **62** 2714
[23] Cai X B and Xuan X F 2004 *Opt. Commun.* **240** 227
[24] Saldaña X I, Contreras-Solorio D A and Lopez-Cruz E 2007 *Revista Mexicana de Física S* **53** 310
[25] Solaimani M, Izadifard M, Arabshahi H and Sarkardei M R 2013 *J. Lumin.* **134** 699
[26] Solaimani M 2014 *Solid State Commun.* **200** 66
[27] Solaimani M 2014 *J. Nonlinear Opt. Phys. Mater.* **23** 1450050
[28] Solaimani M, Ghalandari M and Lavaie L 2016 *J. Opt. Soc. Am. B* **33** 420
[29] Solaimani M 2015 *Chin. Phys. Lett.* **32** 117304
[30] Press W H, Teukolsky S A, Vetterling W T and Flanner B P 2007 *Numerical Recipes: The Art of Scientific Computing*, 3rd edn. (Cambridge: Cambridge University Press)